

Supporting Information

Andrea Amorese^{a,b}, Martin Sundermann^{a,b}, Brett Leedahl^b, Andrea Marino^b, Daisuke Takegami^b, Hlynur Gretarsson^{b,c}, Andrei Gloskovskii^c, Christoph Schlueter^c, Maurits W. Haverkort^d, Yingkai Huang^e, Maria Szlawska^f, Dariusz Kaczorowski^f, Sheng Ran^{g,i}, M. Brian Maple^g, Eric D. Bauer^h, Andreas Leithe-Jasper^b, Philipp Hansmann^{b,j}, Peter Thalmeier^b, Liu Hao Tjeng^b, and Andrea Severing^{a,b,1}

^aInstitute of Physics II, University of Cologne, Zùlpicher StraÙe 77, 50937 Cologne, Germany; ^bMax Planck Institute for Chemical Physics of Solids, Nôthnitzer StraÙe 40, 01187 Dresden, Germany; ^cPETRA III, Deutsches Elektronen-Synchrotron (DESY), NotkestraÙe 85, 22607 Hamburg, Germany; ^dInstitute for Theoretical Physics, Heidelberg University, Philosophenweg 19, 69120 Heidelberg, Germany; ^evan der Waals-Zeeman Institute, University of Amsterdam, 1098 XH Amsterdam, The Netherlands; ^fInstitute of Low Temperature & Structure Research, Polish Academy of Science, 50–950 Wroclaw, Poland; ^gDepartment of Physics, University of California, San Diego, La Jolla, California, USA; ^hLos Alamos National Laboratory, Los Alamos, New Mexico 87545, USA; ⁱPresent address: Physics department, Washington University in St. Louis, St. Louis, Missouri, USA 63130; ^jDepartment of Physics, University of Erlangen - Nuremberg, 91058 Erlangen, Germany

1. Compton

Figure S1(a)-(d) show the experimental NIXS spectra of UFe_2Si_2 (a), UNi_2Si_2 (b), URu_2Si_2 (c) and UPd_2Si_2 (d) over a wide energy range with a coarse energy step size of 0.5 eV (even larger for URu_2Si_2) for different directions of the momentum transfer \vec{q} , $q_{\parallel}[100]$ (blue) and $q_{\parallel}[001]$ (red). The URu_2Si_2 data were obtained in a previous experiment (see Ref. (1, 2)) and here only $\langle \vec{q} \rangle$ averaged signal is shown. The dominant signal arises from Compton scattering and the core-level excitations appear as spikes on top.

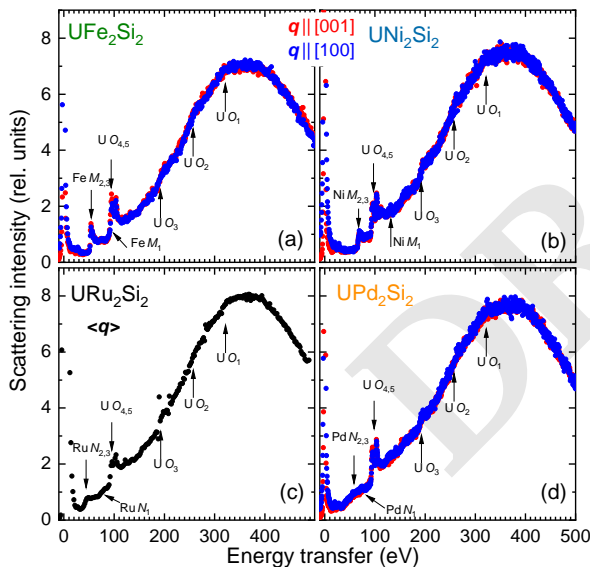


Fig. S1. Experimental wide energy scans at $T < 20$ K covering the peak of the Compton signal of (a) UFe_2Si_2 , (b) UNi_2Si_2 , (c) URu_2Si_2 and of (d) UPd_2Si_2 ; red and blue denote the two different directions of the momentum transfer \vec{q} . The data of different momentum directions are scaled to the Compton peak. The URu_2Si_2 data in panel (c) were acquired in a previous experiment on a different beamline with a larger step size (1, 2) and were averaged over several directions of \vec{q} .

2. Isotropic NIXS spectra of $U f^2$ and $U f^3$

Figure S2 shows the experimental isotropic O4,5 NIXS spectra of UCd_{11} (blue dots) and of UPd_2Si_2 (orange dots), the former very much on the f^3 side and the latter on the f^2 . The line shapes are very different for the different U configurations. In addition, we observe that the UCd_{11} spectrum is shifted towards lower energies by about 0.5–1.0 eV which is typically observed in x-ray absorption studies when comparing configurations with valence states that differ by one; with the lower

valence state lower in energy, see e.g. S. Agrestini *et al.* (3) and references there in.

Figure S2 also displays the theoretical simulations for the isotropic O4,5 NIXS spectra from a pure local $U f^3$ (blue lines) and local $U f^2$ (orange lines) configurations. We can observe that the simulations reproduce very well the experimental spectra, and therefore we can safely infer that the respective configuration assignments of the two compounds are correct. The shaded area denotes the energy range where excitations to the continuum states are becoming more intense. The interference of the atomic-like transitions with these continuum states causes considerable broadening of the spectral features, see e.g. Caciuffo *et al.* (4), which has not been included in the simulations.

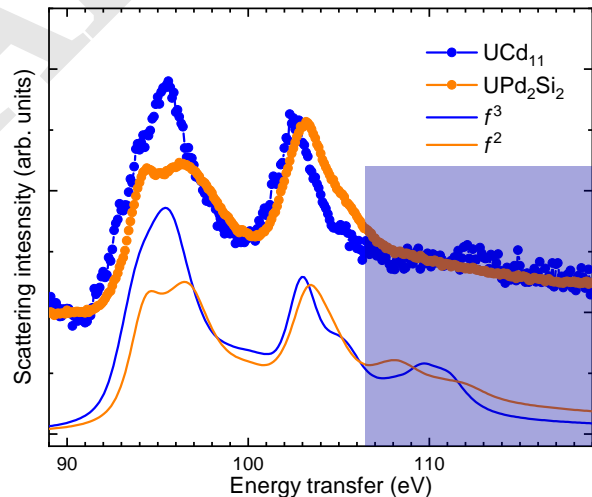


Fig. S2. Isotropic NIXS data of UPd_2Si_2 (orange dots) and of UCd_{11} (blue dots) together with the simulations for a pure $U f^2$ (orange lines) and $U f^3$ (blue lines) configurations. The shaded area indicates the energy regime where excitations to the continuum states are becoming more intense.

3. Properties

Figure S3 summarizes the lattice constants, U transition metal (TM) distances, structure, and ground state properties of the $U M_2\text{Si}_2$ compounds surrounding URu_2Si_2 .

¹Corresponding author: Andrea Severing, E-mail: severing@ph2.uni-koeln.de

3d	I4/mmm a=3.945 c=9.544 Fe $d_{U-TM}=3.095$ PP	I4/mmm a=3.908 c=9.637 Co $d_{U-TM}=3.10$ AF@80K	I4/mmm a=3.970 c=9.523 Ni $d_{U-TM}=3.092$ AF@124,108,40K
4d	I4/mmm a=4.127 c=9.567 Ru $d_{U-TM}=3.164$ HO@17K SC@1.5K	I4/mmm a=4.009 c=10.025 Rh $d_{U-TM}=3.209$ AF@137K	I4/mmm a=4.097 c=10.046 Pd $d_{U-TM}=3.241$ AF@136,≈100,≈75K
5d	I4/mmm a=4.121 c=9.648 Os $d_{U-TM}=3.179$ PP	P4/nmm a=4.076 c=9.783 Ir $d_{U-TM}=3.113$ AF@6K	P4/nmm a=4.192 c=9.687 Pt $d_{U-TM}=3.211$ AF@32K

Fig. S3. Section of the periodic table for the UM_2Si_2 compounds providing the crystallographic structure, the lattice constants, the U–transition metal distances, the ground state properties AF for antiferromagnetic, PP for Pauli paramagnetic, HO for hidden order, SC for superconducting, as well as the temperatures at which the respective transitions take place (5–12).

- H Ptasiewicz-Bak, J Leciejewicz, A Zygunt, Neutron diffraction study of magnetic ordering in UPd_2Si_2 , UPd_2Ge_2 , URh_2Si_2 and URh_2Ge_2 . *J. Phys. F: Met. Phys.* **11**, 1225 (1981).
- KHJ Buschow, DB de Mooij, Structural and magnetic characteristics of several ternary compounds of the type GdX_2Sb_2 and UX_2Sb_2 (X = 3d, 4d or 5d metal). *Philips J. Res.* **41**, 55–76 (1986).
- TT Palstra, AA Menovsky, GJ Nieuwenhuys, JA Mydosh, Magnetic properties of the ternary compounds CeT_2Si_4 and UT_2Si_2 . *J. Magn. Magn. Mat.* **54-57**, 435 (1986).
- T Endstra, GJ Nieuwenhuys, JA Mydosh, Hybridization model for the magnetic-ordering behavior of uranium- and cerium-based 1:2:2 intermetallic compounds. *Phys. Rev. B* **48**, 9595–9605 (1993).
- B Shemirani, et al., Magnetic structure of UPd_2Si_2 . *Phys. Rev. B* **47**, 8672–8675 (1993).
- P Svoboda, P Javorsky, F Honda, V Sechovsky, AA Menocsky, Magnetic phases diagrams in UNi_2Si_2 . *Centr. Eur. J. Phys.* **2**, 397 (2004).
- A Szytuka, L Gondek, M Slaski, B Penc, A Jezierski, Non-magnetic behaviour of UFe_2Si_2 compound. *J. Alloy. Compd.* **44**, 275 (2007).
- T Plackowski, D Kaczorowski, J Sznajd, Magnetic phase diagram and possible Lifshitz critical point in UPd_2Si_2 . *Phys. Rev. B* **83**, 174443 (2011).
- K Kuwahara, et al., High pressure x-ray diffraction study of URu_2Si_2 . *Acta Phys. Polonica B* **34**, 4307 (2003).

4. DFT of UFe_2Si_2 under pressure

Figure S4 shows the result of DFT calculations for UFe_2Si_2 assuming reduced lattice constants to mimic the impact of applied pressure. The conversion of reduced lattice constants to pressure is done on the basis of compressibility data of URu_2Si_2 (13) since data for UFe_2Si_2 are not available. The calculations clearly show that the relative 5f population decreases with increasing pressure, i.e. the $5f^3$ contributes less to the ground state as pressure increases. (Note the absolute 5f occupation numbers should be taken with care since they depend on the calculational basis set and method of counting.)

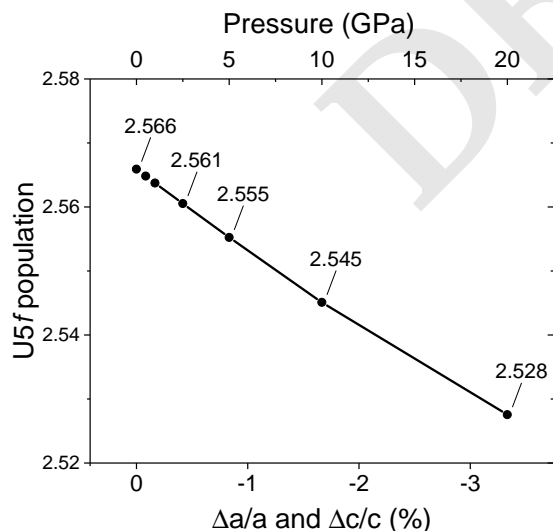


Fig. S4 U 5f population in UFe_2Si_2 as function of $\Delta a/a$ and $\Delta c/c$ in % resulting from DFT calculation using FPLO. The conversion to pressure is based on the compressibility data of URu_2Si_2 (13).

- M Sundermann, et al., Direct bulk-sensitive probe of 5f symmetry in URu_2Si_2 . *Proc. Nat. Acad. Sci. U.S.A.* **113**, 13989 (2016).
- M Sundermann, *PhD thesis*. (University of Cologne), (2019).
- S Agrestini, et al., Probing the $J_{eff}=0$ ground state and the Van Vleck paramagnetism of the Ir^{5+} ions in layered $Sr_2Co_{0.5}Ir_{0.5}O_4$. *Phys. Rev. B* **97**, 214436 (2018).
- R Caciuffo, et al., Uranium 5d – 5f electric-multipole transitions probed by nonresonant inelastic x-ray scattering. *Phys. Rev. B* **81**, 195104 (2010).